Marine Pollution Bulletin 185 (2022) 114359

Contents lists available at ScienceDirect

Marine Pollution Bulletin

journal homepage: www.elsevier.com/locate/marpolbul

Spatial distribution of pollution levels and assessment of benthic foraminifera in Apapa-Badagry Creek, Nigeria

Olugbenga T. Fajemila[a], Michael Martínez-Colón[b,*], Ivory Council[b], Silvia Spezzaferri[c]

[a] Department of Geological Sciences, Osun State University, Osogbo, Nigeria
[b] School of the Environment, Florida A&M University, Tallahassee, FL, USA
[c] Department of Geosciences, University of Fribourg, Fribourg, Switzerland

ARTICLE INFO

Keywords:
Heavy metals
Fractionation
Meiofauna
Bioavailability
Nigeria

ABSTRACT

The Apapa and Badagry creeks in Nigeria are a corridor of long-term anthropogenic activities, including mangrove removal, urban expansion, and industrialization. Consequently, this uncontrolled development led to the release of untreated effluents and wastes, which resulted in sediment and water quality degradation. This area has the highest degree of pollution (Enrichment and Contamination Factors) especially north of Tincan Island where potentially toxic element (PTE) depocenters occur. Our data shows that salinity and pH are the two main factors favoring foraminiferal distributions, but the sediments in the depocenters with the highest degree of PTE pollution are barren of foraminifera. Bioavailable sediment-bound PTEs have been found to negatively impact the assemblage distribution and diversity. It is important to highlight that dissolved phosphorous was the only PTE that negatively impacted species richness. This study highlights the significance of implementing PTE bioavailability as an integral part of ecosystem functioning in all nearshore environments.

1. Introduction

Estuaries are transitional environments that combine the physiochemical characteristics of their adjacent landforms and water bodies. In estuarine environments, the interchange between both fresh and saltwater realms occurs on a regular basis as controlled by the tidal regime (e.g., diurnal, semi-diurnal). These ecotones are brackish shallow-water marginal ecosystems impacted by both natural and human disturbances. Ecotones serve as economically significant places for aquaculture, harbor development, urban expansion, and a variety of other activities that contribute to the general economic well-being of the local population and, in some cases, the whole country (e.g., Lagos in Nigeria). As a result of these activities, most nearshore habitats have been severely polluted and degraded (e.g., Frontalini and Coccioni, 2008; Coccioni et al., 2009; Martins et al., 2010; Martínez-Colón et al., 2018; Elshanawany et al., 2018; El Kateb et al., 2018, 2020; Fajemila et al., 2022a, 2022b; Al-Enezi et al., 2022). The introduction of noxious compounds into these ecosystems from untreated industrial effluents and sewage as well as domestic wastes, has the potential to cause a temporal or permanent shift in the natural ecological conditions required by meiofaunal populations (Fajemila et al., 2022b).

It is well known that the fate and transport of pollutants like potentially toxic elements (PTEs) are controlled by the physiochemical characteristics of the sediments and water column (see Martínez-Colón et al., 2009). These parameters will vary by location (open marine, estuary, lagoonal, etc.). Estuaries serve as sinks for numerous types of pollutants. These environments typically experience changes in salinity, pH, and dissolved oxygen depending on the proximity to fresh water sources and tidal turnover, among others. In extreme cases, dredging activities have caused permanent stratification which has produced permanent anoxic conditions (Martínez-Colón et al., 2018; Fajemila et al., 2022b), altering the chemistry of the water column and sediments.

Along the Gulf of Guinea in Nigeria, the Apapa-Badagry Creek (ABC) in the Lagos Harbor (LH) is known for being impacted by anthropogenic activities. Numerous authors describe that the ABC receives pollutants from multiple point- and non-point sources derived from hydrocarbon production, urban activities, and sewage, among others (Don-Pedro et al., 2004; Obi et al., 2016). Recently, Fajemila et al. (2022b) reported that these sources of pollution have impacted the quantity and quality of organic matter being preserved in the harbor. This is an important observation since the level of PTE bioavailability is dependent upon sediment type and organic matter content (e.g., Martins et al., 2020; Martínez-Colón et al., 2018; Barik et al., 2022; Fajemila et al., 2022a).

Benthic foraminifera are cosmopolitan shelled protists with a very

* Corresponding author.
E-mail address: michael.martinez@famu.edu (M. Martínez-Colón).

https://doi.org/10.1016/j.marpolbul.2022.114359
Received 13 July 2022; Received in revised form 6 November 2022; Accepted 9 November 2022

short life cycle. The distribution and diversity of this meiofaunal group in estuaries and other comparable settings around the world have been recorded in several studies (e.g., Langer et al., 2016a, 2016b; Fajemila and Langer, 2016, 2017; Gildeeva et al., 2021; Sariaslan and Langer, 2021). More importantly, the physiochemical gradients (e.g., pH, sediment texture) of their microhabitats (as shown by Jorissen, 1999), especially at the sediment-water interface, plays an integral role in the ecology and distribution of the foraminifers. For example, in Lagos Lagoon (LL), Fajemila et al. (2020) described foraminiferal wall structure (e.g., calcareous, agglutinated) distributions based on salinity and sediment properties (e.g., texture). Other mitigating factors such as temperature changes, eutrophication, nitrification, organic matter quality and quantity, and turbidity help defining the spatio-temporal variations in foraminiferal distribution, abundance, and diversity. Some benthic foraminifers are typically anchored to a substrate (e.g., *Homotrema*) or have limited mobility (e.g., Langer, 1993; Davaud and Septfontaine, 1995), making them vulnerable to natural or anthropogenic perturbations. Aside from having excellent preservation potential in sediments (e.g., Langer and Lipps, 2006; Fajemila et al., 2015), these organisms react quickly to short- and/or long-term environmental changes. Their ecological responses to stressors (e.g., salinity changes, pollutants) have been documented since the 1960s (see Sen Gupta, 2013). However, new evidence suggests that the buildup of pollutants is powerful enough to modify microhabitats and affect their assemblage's diversity and abundance. These ecological changes have been used extensively as bioindicator tools to better understand the impact of PTEs (see Yanko et al., 1998; Pinto et al., 2003; Bergamin et al., 2009; Martins et al., 2015; Martins et al., 2016; Amao et al., 2019; Guo et al., 2020; Li et al., 2021; Fajemila et al., 2022a; Dimiza et al., 2022; Cavaliere et al., 2021). Unfortunately, most of these studies have used total PTE concentrations instead of considering the potential bioavailability of these pollutants in response to the foraminifers. However, there is a great risk of misinterpretation when relying only on the total PTE concentration since the overestimation will produce either false "positives" or "negatives". PTEs found adsorbed to sediments (exchangeable F1 fraction) and complexed with organic matter (oxidizable F4 fraction) are considered more readily bioavailable to foraminifers (Martínez-Colón et al., 2009, 2017, 2018; Fajemila et al., 2022a).

The purpose of this study is to understand how PTE bioavailability affected benthic foraminifers in the ABC in Lagos harbor. The following objectives were met: (1) the Contamination factor, enrichment factor, and ecological risk index pollution indices were calculated to assess the level of environmental degradation; and (2) the ecological response of benthic foraminifera was used to assess the importance of PTE bioavailability.

2. Materials and methods

2.1. Study area and sampling

The ABC, in southwestern Nigeria, is located between longitudes 3° 23′ and 3° 40′ E and latitudes 6° 22′ and 6° 38′ N (Fig. 1) and serves as a hub for many local and regional economic activities. This estuary is linked with the Atlantic Ocean through the Commodore Channel (CC), and is regularly refreshed by the riverine domains from the hinterland. This environment is relatively shallow, with depths ranging from 1.5 to 8 m. The bottom pH is acidic (7.31–7.87) and salinity ranges between 0.73 and 17.50, making the LH an oligohaline to mesohaline environment according to the classification of Montagna et al. (2013). The water column is practically homogenous with respect to temperature and pH but at some stations (3–5, 17–18, 22, 26–28), the water is slightly stratified in relation to salinity. A similar observation was documented by Vijverberg et al. (2012) who reported a halocline at ~2.5 m depth at the Apapa Creek (AC) and Badagry Creek (BC) confluence east of Tincan Island. Some of these stream channels pass through heavily populated settlements and are therefore prone to contamination from sewage and other untreated effluents. Along the fringes of the estuary are red mangrove trees (*Rhizophora racemosa*) most of which were removed for urban and industrial development, where industries such as petrochemicals, textiles, breweries, food processing, and many more are on the rise. Furthermore, the LH is housed in the western part of the estuary. This is the largest seaport in the country for international trade and other maritime activities. Petroleum products are by far the largest trade in the port with many large reservoir tanks (e.g., holding depots) now replacing the mangroves at the edges of the estuary. Sand mining, fishing, and dredging are common daily activities within the river channels of the ABC (see Don-Pedro et al., 2004; Ajao, 1996; Fajemila et al., 2022b).

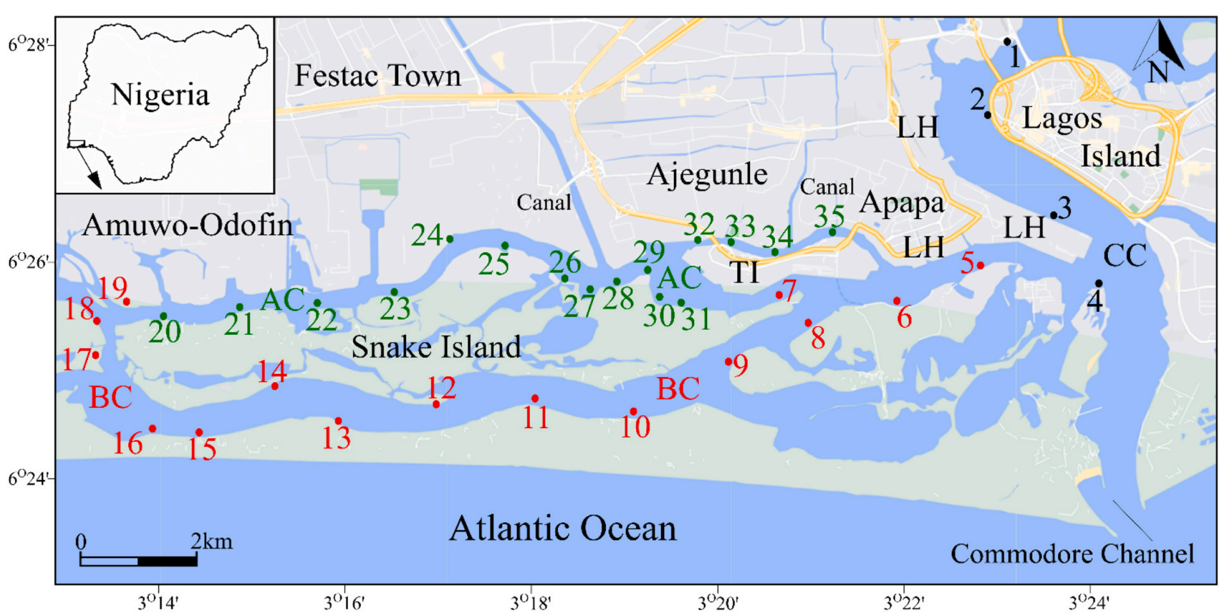

Fig. 1. Study area sampling sites (1–35) within the Apapa-Badagry Creek (Modified from Google Map: https://earth.google.com/web). LH = Lagos Harbor; CC (black color) = Commodore Channel; BC (red color) = Badagry Creek; AC (green color) = Apapa Creek; TI = Tincan Island. (For interpretation of the references to color in this figure legend, the reader is referred to the web version of this article.)

The ABC was sampled following the FoBIMO protocol of Schönfeld et al. (2012) however, no replicates could be taken due to time constraints. Sediment samples were collected from 35 stations with an Ekman-Birge box corer (15 × 15 × 30 cm) using a small boat. The study area was divided in three sectors of the ABC according to Fajemila et al. (2022b); the CC, AC and BC water bodies (Fig. 1). The CC contains the sampled sites that could be affected by regular dredging. The AC (from LH to Amuwo-Odofin; Fig. 1) is lined with large petroleum tanks and harbor activities coupled with effluents from poor sewage systems and polluted canals and streams from nearby high-density residential estates and communities. The BC is bordered by fishing villages, mangrove marshlands, recreational lands, and other governmental institutions, as well as sand mining activities within the river channel (western end of the creek).

2.2. Benthic foraminiferal and grain-size analyses

Sediments samples from 35 sites were treated with an ethanol/Rose Bengal solution (1 L/2 g) and washed through the >32 μm mesh sieve after soaking for more than two weeks. Since in low salinity environments like the ABC benthic foraminifera can be very small, the >32 μm size was used to retain the smallest specimens. The total assemblage (living + dead) of up to 308 benthic foraminiferal specimens were recovered from 25 sites while others were barren to nearly barren. Living (stained) assemblages were reported by Fajemila et al. (2022b). In this study, we have applied the taxonomic scheme from foraminiferal studies in the Gulf of Guinea and other parts of Africa (e.g., Langer et al., 2016a, b; Fajemila and Langer, 2016, 2017; Fajemila et al., 2020, 2022b).

The grain-size analysis was carried out on all the sediment samples following standard procedures as described by Fajemila et al. (2022b). To determine the overall texture of the sediments, the graphic mean (M_Z), which is based on three percentiles, was adopted.

2.3. Geochemical analyses

Details of the measurements of the total organic carbon (TOC) and calcium carbonate (CO_3) percent calculation are in Fajemila et al. (2022b). To assess the level of pollution in this study, the PTE concentrations from bulk sediments were extracted. Two aliquots of 0.5 g and 1 g were used to extract "pseudo-total" (referred to as "total" in this article) and sequentially extracted PTES respectively. An agate mortar and pestle were used to crush the sediments from each sampled site into a powder to maximize the digestion process by increasing the surface area of the sediments. For the total extraction, an aqua regia solution was made using a 3:1 ratio of concentrated and trace metal grade acids (HNO_3:HCl). The aqua-regia and sediment mixture were placed in Teflon "bombs" and left partially sealed for 24 h to allow the exothermic reaction to decrease in intensity. Subsequently, the "bombs" were sealed and heated in a microwave following the EPA 3051A method (U.S. EPA, 2007). After digestion, the extract was filtered into 50 mL Falcon tubes using MCE filters (0.22 μm) attached to a syringe and diluted to 30 mL with 3 % trace metal grade HNO_3.

For the sequential extraction methods, the protocols of Tessier et al. (1979) are based on "operational" bioavailability or how easily extracted are the PTEs. Five fractions were described with the exchangeable (F1) fraction being the most bioavailable given that PTEs were easily extracted with salts (e.g., Magnesium chloride, Sodium acetate) while strong acids (Hydrofluoric) are used to extract the least bioavailable PTEs from the residual (F5) fraction. As described by Martínez-Colón et al. (2018) and Fajemila et al. (2022a), the exchangeable (F1) and oxidizable (F4) fractions are considered the most bioavailable to the foraminifers. Although for the latter, stronger acids and oxidizers were implemented, the PTEs in this fraction are important given that foraminifers indeed rely on organic matter as a food source. After the F1 and F4 digestions, the extracts were also filtered and diluted to 30 mL with 3 % trace metal grade HNO_3. All extracts were analyzed using an Inductively Coupled Plasma Optical Emission Spectrometry (ICP-OES) for Co, As, Se, Pb, Cr, Al, Fe, Cu, Cd, Ni, and Zn. For concentrations found below the detection limit (BDL) of the instrument, we reported half of the detection limit (0.001 mg/L). As suggested by Parker and Arnold (1999), this approach rejects the potential of false zeros and considers the actual presence of the PTE.

The water samples were collected very close to the sediment surface at each sample station with a horizontal water sampler and stored in an acid-washed Nalgene bottles. At each site, 120 mL of water was collected and acidified (pH = 1) by adding 5 mL of concentrated HNO_3 to avoid precipitation of coordination complexes. Subsequently the samples were stored at 4 °C until analyzed. Elemental analyses of the water samples for Cl, Na, Cd, Cr, Fe, P, V, Mn, Co, Ni, Pb, As and Zn concentrations were carried out using the Spectro Arcos Inductively Coupled Plasma Optical Emission Spectrometry (ICP-OES).

For this study we took into consideration the percent mud (%mud), total organic carbon (TOC), percent carbonate content (CO_3), foraminiferal taxa (total assemblage), species richness, and the Shannon Index data as reported by Fajemila et al. (2022b). The concentration factor (CF), enrichment factor (EF), and the ecological risk index (RI) were calculated for the PTEs of interest, using total concentrations to assess the level of anthropogenic input. A more detail description of the calculations is found in Fajemila et al. (2022a).

2.4. Data analysis

Given the low abundance of foraminifers, adjustment was made to eliminate those species that were not present in at least 8 % of the samples ending with 22 species. A Q-mode clustering technique with the paired group algorithm using the Bray-Curtis dissimilarity was performed to determine the structure in the foraminiferal data. This mode of clustering grouped together samples stations with similar benthic foraminiferal assemblages and revealed a categorization of environmental signatures that are shown in a hierarchical dendrogram. To determine the ecological signature of the foraminifers the following were used:

$$\text{Species Richness}: \ S = \text{number of species per sample} \tag{1}$$

$$\text{Shannon } Index: \ H(S) = -\Sigma\, pi \times ln(pi) \tag{2}$$

where pi if the relative abundance of a foraminiferal species (Shannon, 1948).

To determine the level of environmental contamination by the PTEs, the following three indices were calculated (see detail descriptions in Turekian and Wedepohl, 1961; Liaghati et al., 2003; Fajemila et al., 2022a):

$$\text{Enrichment } Factor: \text{EF} = \left(C_i/C_{\text{ref}}\right)\text{sample}/\left(C_i/C_{\text{ref}}\right)\text{crust} \tag{3}$$

where C_i is the PTE concentration of interest in the sample and C_{ref} is the confentration of the normalizing element.

$$\text{Concentration } Factor: \text{CF} = \text{CF}_{\text{PTE}}/C_{\text{background}} \tag{4}$$

where CF_{PTE} is the concentration of the PTE of interest and $C_{background}$ is the concentration of the same PTE found in shale.

$$\text{Ecological Risk } Index: \text{RI} = \Sigma\text{Er}_{\text{PTE}}, \text{ where } \text{Er}_{\text{PTE}} = \text{Trf}^{*}\ \text{CF} \tag{5}$$

where Trf is the toxic response factor and CF is the concentration factor of the PTE of interest.

A Pearson correlation on square-root transformed data was done using %mud, TOC, and CO_3, total PTE concentration, F1 (acid-soluble), F4 (oxidizable), S, and H(S) including the normalized (to dry mass in grams) foraminiferal dead assemblage. This was done using the Paleontological Statistical (PAST- v. 4.08) software (Hammer et al., 2001).

The stations that had zero foraminiferal counts (e.g., barren) were excluded from the cross-correlation. The excluded stations were 2, 7, 9, 14, 19, 22–24, 34–35. Contour maps were plotted using Surfer® software (v. 22.1.151) (www.goldensoftware.com) to illustrate potential hot spots of pollution, distribution of PTEs, and key foraminiferal taxa.

3. Results

3.1. Benthic foraminifera

A total of 5756 foraminiferal individuals representing 87 species and belonging to 37 genera were picked and identified. Hyaline perforate taxa were the most dominant wall group making 61.5 % of the total count. They were found at almost all the sample sites wherever foraminifera were present. Agglutinated taxa were next in dominance with about 36.6 % population. These are very rare within the CC but are prominent at the innermost brackish water sites in AC and BC. The porcelaneous wall taxa are limited to those sample sites within and very close to the CC making up to 1.9 % of the total foraminiferal abundance. The H(S) index ranged between 0.12 and 2.09 in individual samples (Table 1). The species richness was higher in the CC sites than anywhere in the ABC. In general, S decreased westwards along with both AC and BC (Table 1).

Species of *Ammonia* dominated the assemblage in stations 6, 11, 25, 29–30, most of which are in the AC (Fig. 2). They make up approximately 50 % of the total population at these stations. Similarly, *Ammotium* species, which are a little <30 % of the total count, are equally dominant within the BC stations (12, 13. 16–18; Fig. 2). The porcelaneous taxa are represented by *Quinqueloculina* species and are prominent in station 3 in the CC. Generally, species count increased eastwards towards the more saline CC stations because they are influenced by the Atlantic Ocean. Only 10 species were found to be living (stained) in the sediments as reported by Fajemila et al. (2022b). Given that *Ammonia aoetana* (total of 2258 counts) and *Ammotium salsum* (1617 counts) were the only two species dominating the assemblage, these were used in the cross-correlation analysis.

The Q-mode clustering with the paired group algorithm using the Bray-Curtis dissimilarity was employed to determine the structure in the foraminiferal data set. Samples with similar faunal assemblages were grouped by this technique to reveal a typology of environmental indicators embedded in a hierarchical dendrogram. The cluster analysis was based on absolute abundance data of the 22 most abundant species, which make up ~98 % of the total population of foraminifera counted (see Supplemental Material- Appendix A). Six clusters were recognized in the dendrogram with the phenon line placed at 0.45 similarity index (Fig. 3). Cluster A consists only station 3 located in the CC, and has the highest number of foraminiferal species in the ABC area. *Cribroelphidium mirum*, *Nonion fabum*, *Bolivina* sp. 1, *Hanzawaia* cf. *H. nipponica* and

Table 1
Parameters measured in the Apapa-Badagry Creek and details of the sampled sites. SS = Sample station; M_Z = Graphic mean; S = Species richness; H(S) = Shannon Index (modified from Fajemila et al., 2022b).

SS	Depth (m)	Latitude	Longitude	TOC (wt%)	$CaCO_3$ (%)	Mud (%)	M_Z	Benthic foraminifera				
								S	H(S)	Dead	Living	Total
Commodore Channel (CC)												
1	1.3	06 28′ 01.5″	003 22′ 57.1″	0.67	1.80	12.48	2.85	20	1.70	288	31	319
2	1.6	06 27′ 22.7″	003 22′ 50.2″	0.17	4.22	3.98	1.64			Barren		
3	8.5	06 26′ 26.1″	003 23′ 22.9″	1.95	4.49	69.79	4.05	53	2.86	344	16	360
4	1.5	06 25′ 48.0″	003 23′ 50.3″	0.06	0.58	3.63	1.67	22	2.30	314	4	314
Badagry Creek (BC)												
5	4.7	06 25′ 57.9″	003 22′ 41.6″	1.34	1.21	17.40	3.30	25	2.06	342	14	356
6	1.8	06 25′ 40.2″	003 21′ 56.9″	1.40	1.43	27.79	3.18	28	1.99	344	70	414
7	1.8	06 25′ 40.4″	003 20′ 51.5″	0.23	0.29	3.00	2.04			Barren		
8	2.4	06 25′ 22.9″	003 21′ 06.9″	0.41	0.41	12.19	1.87	6	1.21	82	2	84
9	2.5	06 25′ 05.7″	003 20′ 27.2″	0.33	0.53	7.51	2.00			Barren		
10	1.8	06 24′ 38.5″	003 19′ 30.6″	2.19	2.13	60.95	3.95	3	1.08	45	1	46
11	1.2	06 24′ 43.3″	003 18′ 35.9″	4.66	1.83	74.34	4.17	6	1.1	303	0	303
12	1.5	06 24′ 42.4″	003 17′ 40.9″	0.21	0.21	2.17	1.13	5	0.52	330	33	363
13	1.9	06 24′ 32.9″	003 16′ 47.2″	1.60	0.98	13.27	1.98	4	0.43	310	18	328
14	1.4	06 24′ 52.5″	003 16′ 11.7″	0.51	0.53	4.59	1.87			Barren		
15	6.5	06 24′ 24.7″	003 15′ 29.7″	1.70	0.90	25.00	2.64	4	0.40	109	2	111
16	1.4	06 24′ 26.7″	003 15′ 04.0″	1.67	1.23	41.39	2.89	4	0.37	251	16	267
17	5.2	06 25′ 12.6″	003 14′ 39.8″	4.86	1.78	76.66	4.32	11	1.37	303	9	312
18	2.2	06 25′ 28.2″	003 14′ 34.8″	5.84	2.49	79.59	4.47	5	0.41	309	11	320
19	1.3	06 25′ 37.5″	003 14′ 47.6″	0.46	1.17	5.22	2.03			Barren		
Apapa Creek (AC)												
20	6.3	06 25′ 31.2″	003 15′ 10.5″	0.75	0.54	11.55	2.08	4	1.19	25	0	25
21	6.7	06 25′ 32.7″	003 15′ 50.9″	2.34	0.81	18.30	3.14	3	0.28	32	1	33
22	4.1	06 25′ 37.6″	003 16′ 34.4″	0.06	0.16	3.12	1.62			Barren		
23	4.8	06 25′ 43.2″	003 17′ 18.2″	1.49	1.09	16.44	2.73					
24	4.5	06 26′ 10.9″	003 17′ 48.8″	0.17	0.21	5.29	1.38					
25	2.5	06 26′ 09.3″	003 18′ 19.2″	6.17	1.86	75.60	4.36	4	0.30	224	6	230
26	1.2	06 25′ 54.1″	003 18′ 52.6″	0.66	0.43	4.53	2.16	7	1.26	292	23	315
27	5.2	06 25′ 44.4″	003 19′ 06.6″	3.78	1.38	95.14	4.80	5	0.96	275	1	276
28	6.1	06 25′ 40.9″	003 19′ 21.4″	0.75	0.51	8.58	1.07	5	0.71	221	11	232
29	5.5	06 25′ 56.2″	003 19′ 38.1″	0.96	0.61	12.86	2.59	9	0.95	380	102	482
30	1.5	06 25′ 42.6″	003 19′ 45.5″	3.96	2.13	61.93	3.80	5	0.12	302	19	321
31	1.7	06 25′ 38.7″	003 19′ 55.7″	0.27	0.34	3.24	1.58	4	1.06	25	0	25
32	1.2	06 26′ 14.0″	003 20′ 09.1″	0.64	1.10	4.44	2.06	3	0.82	75	2	77
33	2.6	06 26′ 12.4″	003 20′ 22.9″	7.73	2.70	5.03	1.38	3	0.35	145	3	148
34	3.1	06 26′ 06.4″	003 20′ 48.3″	1.93	0.77	14.15	2.25			Barren		
35	1.4	06 26′ 17.0″	003 21′ 21.3″	8.94	2.20	85.25	4.70					

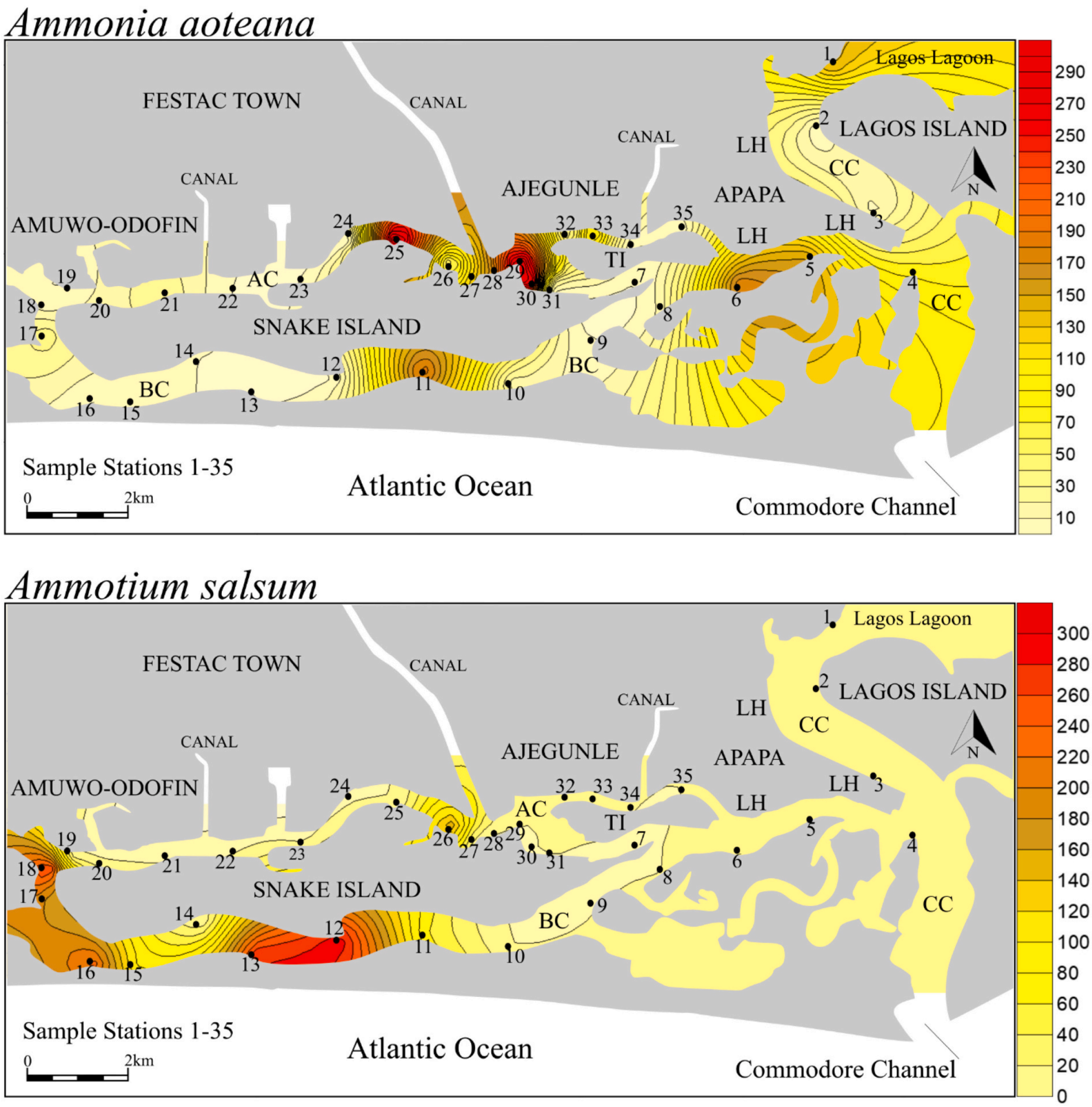

Fig. 2. Spatial distribution of the two most abundant species of foraminifera; (A) *Ammonia aoteana* and (B) *Ammotium salsum* in the ABC. Vertical scale bar: absolute number of foraminiferal counts.

Quinqueloculina spp., among others, make up higher percentages in this cluster. Cluster B is distinct with abundant *A. salsum* along BC (stations12–13, 15–18) and in station 26 in AC (Figs. 3 and 4). Cluster C comprised stations 20, 21, 31 and 32 within the AC. These stations have very low population of *A. aoteana*. Cluster D comprised only two stations (8, 10) that have significant numbers of *Trochammina* sp1. but with very low total counts of other species. Cluster E comprises two subclusters that are defined on the presence of *Ammonia* species. Station 27, which is the only sample site within subcluster Ei, contained a high population of *Ammonia* sp. 1 (Fig. 3). Subcluster Eii consisted of sites with very high abundance of *A. aoteana* (Figs. 2 and 4) along AC and CC. Sample stations 25 and 29–30 in this cluster contained 94, 77 and 98 % of *A. aoteana,* respectively. Both *N. fabum* and *Pararotalia sarmientoi* are very abundant in site 4 from Cluster F, located in the CC, which has the greatest marine influence, like Cluster A. The presence of *Textularia* sp. 1 and the absence of many *Quinqueloculina* species distinguishes Cluster F from the other cluster groups.

3.2. Sediments

The %mud varied from 2.15 to 95.14 % with the highest percentages found along AC as reported by Fajemila et al. (2022b). The most dominant M_z reported were medium sand (CC and BC) and fine sand (AC). The amount of TOC was relatively uniform ranging from 0.17 to 8.94 % with the highest content found along AC. Both %mud and TOC increased from east to west along BC and from west to east along AC. No pattern was reported along CC (Table 1) and no distinct spatial pattern was reported for CO_3 by Fajemila et al. (2022b).

3.3. Sedimented PTEs

For this study, a total of 11 PTEs (Co, As, Se, Pb, Cr, Al, Fe, Cu, Cd, Ni, Zn) were analyzed for both total and sequentially extracted concentrations (see Supplementary Material-Appendix B). The concentrations of As, Se, and Cd were found to be below detection limit (BDL) in the total, F1 and F4 fractions. In addition, Cr_{F1} and Ni_{F1} were excluded from any

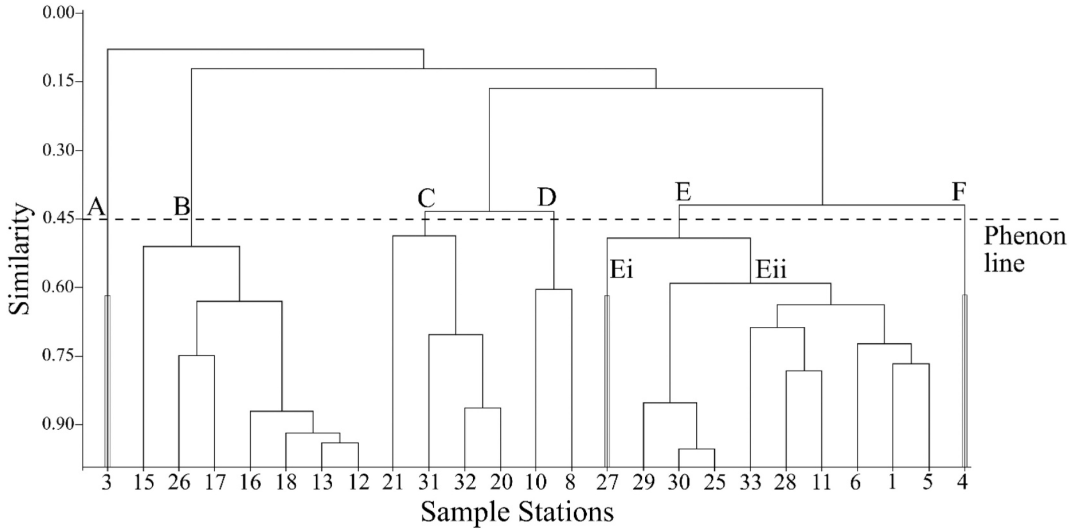

Fig. 3. Q-mode cluster diagram of sample sites showing the six (A–F) clusters including subclusters Ei and Eii. Dashline = phenon line at 0.45 similarity.

Fig. 4. Photomicrographs of some indicator foraminiferal species characterizing the clusters in the ABC. 1: *Ammotium salsum* (side view); 2–5: *Trochammina* sp. 1 (2, 5 –umbilical view; 3, 4 – spiral view); 6–8: *Ammonia aoteana* (6 – spiral view; 7 – apertural view; 8 – umbilical view). Rose Bengal stained (living) (4–8). (For interpretation of the references to color in this figure legend, the reader is referred to the web version of this article.)

statistical analysis given that their concentrations in over 60 % of the samples were BDL. The range of total PTE concentrations in ABC are as follows: Co (0.3–29.64 mg/kg), Pb (3.06–147.60 mg/kg), Cr (3.36–122.70 mg/kg), Al (0.13–3.44 %), Fe (0.8–2.73 %), Cu (2.82–116.08 mg/kg), Ni (0.54–25.98 mg/kg), and Zn (2.04–1423.80 mg/kg). Slight differences are observed when looking at the BC and AC sectors separately. For example, a relative increasing trend from east to west along BC was observed for all PTEs except for Pb (Fig. 5). Although most of the PTEs have EF values <2 ("unpolluted/slightly" polluted) in most stations, no discernable distribution pattern was observed. Only stations 11 was categorized as "extremely" polluted (5 < EF < 20) for Co-Cr-Fe-Zn and in station 5 was for Pb respectively. All stations had both CF <1 and RI <150 indicative of "unpolluted/slightly" polluted conditions.

In the AC, all the PTE total concentrations increased from west to east station 35, which is barren of foraminifers, served as a depocenter along AC in relation to the highest concentrations of Pb (25-fold increase), Cr (15-fold), Cu (35-fold), Ni (28-fold), and Zn (230-fold) followed by 33 and 34 (barren). Appendix C (see Supplementary Material) shows most PTEs had EF values <2 with no discernable distribution pattern. Station 35 is considered "high extreme" (20 < EF < 40) for Pb and "moderately" (2 < EF < 5) to "severely" (5 < EF < 20) polluted for Cr and Cu respectively. Station 33 is considered "severely" polluted for Co and "extreme" (EF > 40) for Zn. The CF values were mostly <1 except for Pb and Zn (CF > 6; "extreme" pollution) in stations 35 and 33, respectively. Like BC, all RI were < 150 indicative of "unpolluted/slightly" polluted conditions.

Apart from Cu, most PTEs were found with the highest concentrations in the F4 fraction. The range of values in ABC for each of the two fractions are as follows: Co_{F1} (0–0.60 mg/kg) and Co_{F4} (0.03–15.18 mg/kg); Pb_{F1} (0.1–2.55 mg/kg) and Pb_{F4} (0.50–15.48 mg/kg); Cr_{F4} (0.54–21.96 mg/kg); Al_{F1} (0 %) and Al_{F4} (0–0.25 %); Fe_{F1} (0–0.01 %)

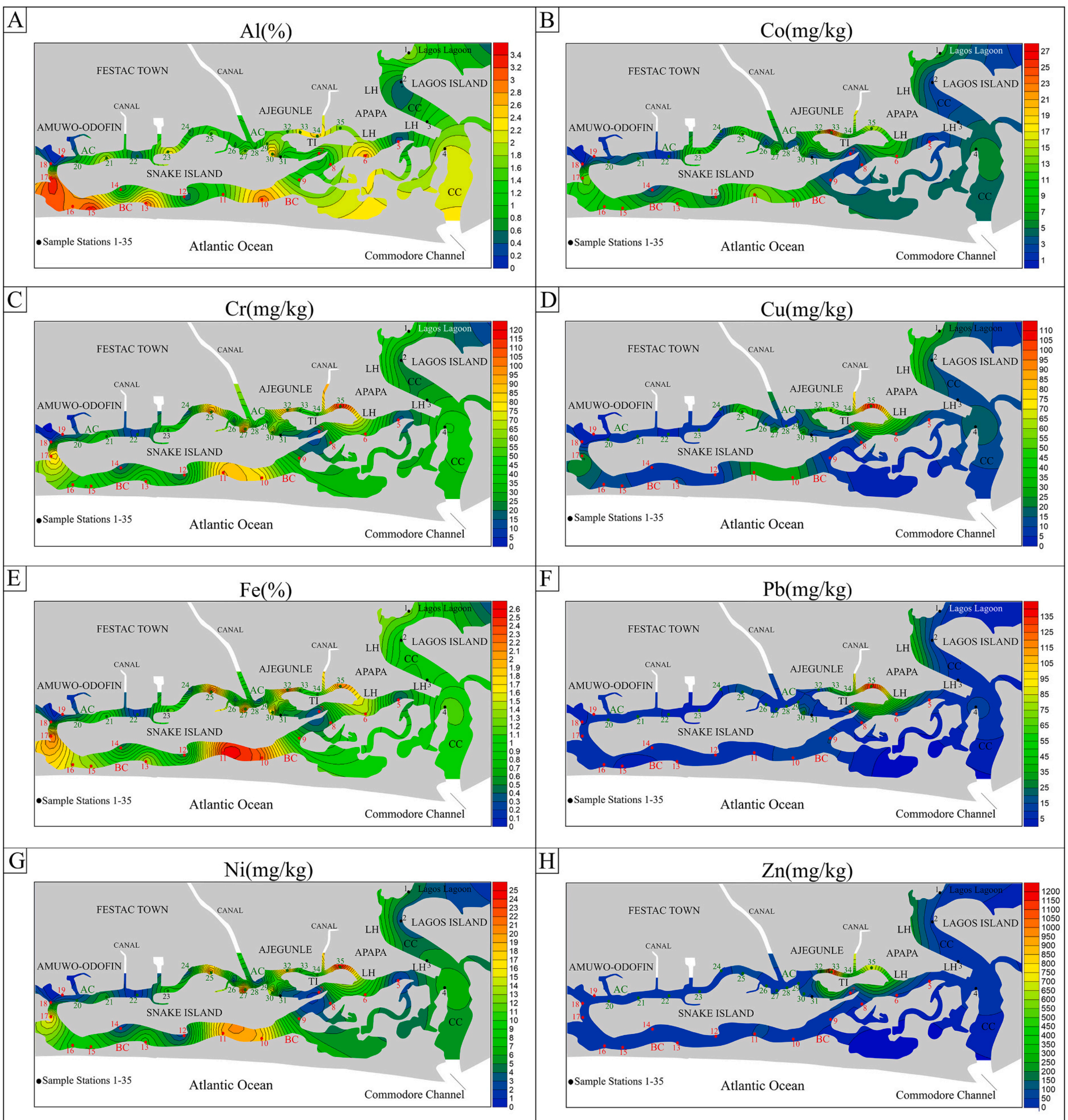

Fig. 5. Heat maps showing the spatial distribution of the total PTE concentrations across the Apapa-Badagry Creek. (A): Aluminum (Al), (B): Cobalt (Co), (C) Chromium (Cr), (D): Copper (Cu), (E): Iron (Fe), (F): Lead (Pb), (G): Nickel (Ni), (H): Zinc (Zn).

and Fe_{F4} (0–0.28 %); Cu_{F1} (0.57–121.83 mg/kg) and Cu_{F4} (0.60–89.40 mg/kg); Ni_{F4} (0.12–10.26 mg/kg); and Zn_{F1} (0.21–44.76 mg/kg) and Zn_{F4} (1.38–1853.40 mg/kg) (see Supplementary Material-Appendix B). Co_{F1}-Pb_{F1}-Al_{F1}- Fe_{F1}-Cu_{F1}-Zn_{F1} showed a relative decrease in concentration along BC from east to west while Cu_{F1} and Zn_{F1} had opposing trends along AC from west to east (Fig. 6). No apparent spatial distribution was observed in the F4 fraction except for Cu_{F4}-Ni_{F4}-Zn_{F4}, which showed a slight increase from west to east along AC (Fig. 7). Like what was observed with the total concentrations, station 35 also served as a depocenter along AC in relation to the highest concentrations of Pb_{F4} (1000-fold increase), Cr_{F4} (40-fold), Al_{F4} (138-fold), Cu_{F4} (5900-fold) and Ni_{F4} (85-fold).

3.4. Water PTE concentrations

As expected, the PTE concentrations from the bottom water column were much lower (μg/L) than in the sediments (see Appendix B). The range of values for each PTE is as follows: Co (0.81–9.03), As (0.73–5.51), Pb (16.51–88.90), Cr (7.45–48.86), Cu (6.33–29.47), Cd (0.71–6.39), Ni (4.76–25.68), P (111.50–297.60), and Zn (37.1–180.10). In the case of Al and Fe, these concentrations were above range while Se was BDL. No apparent spatial distribution was observed along BC except for Co and Ni which showed relative increases from east to west. On the other hand, Co and Cu showed slight decreases in concentration from west to east along AC. Station 5 which is in proximity to the "confluence" between CC and BC, had the highest Co, Cr, and Ni concentrations.

3.5. Pearson correlation matrix

The three sectors CC, AC, and BC (see Supplemental Material-Appendix D) was analyzed separately given their differences in the

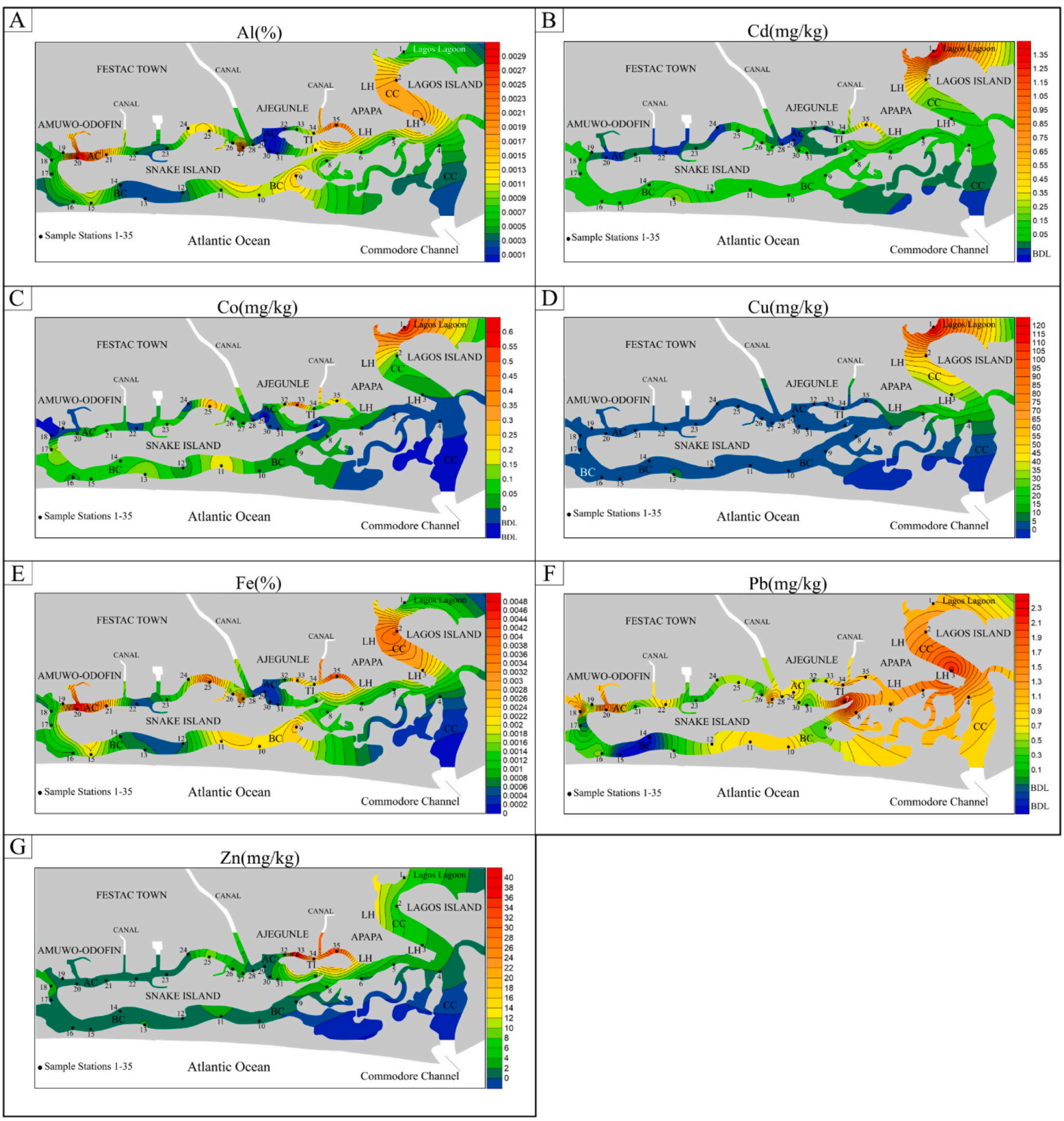

Fig. 6. Heat maps showing the spatial distribution of the F1 exchangeable fractions of PTEs across the Apapa-Badagry Creek. (A): Aluminum (Al), (B): Cadmium (Cd), (C): Cobalt (Co), (D): Copper (Cu), (E): Iron (Fe), (F): Lead (Pb), (G): Zinc (Zn).

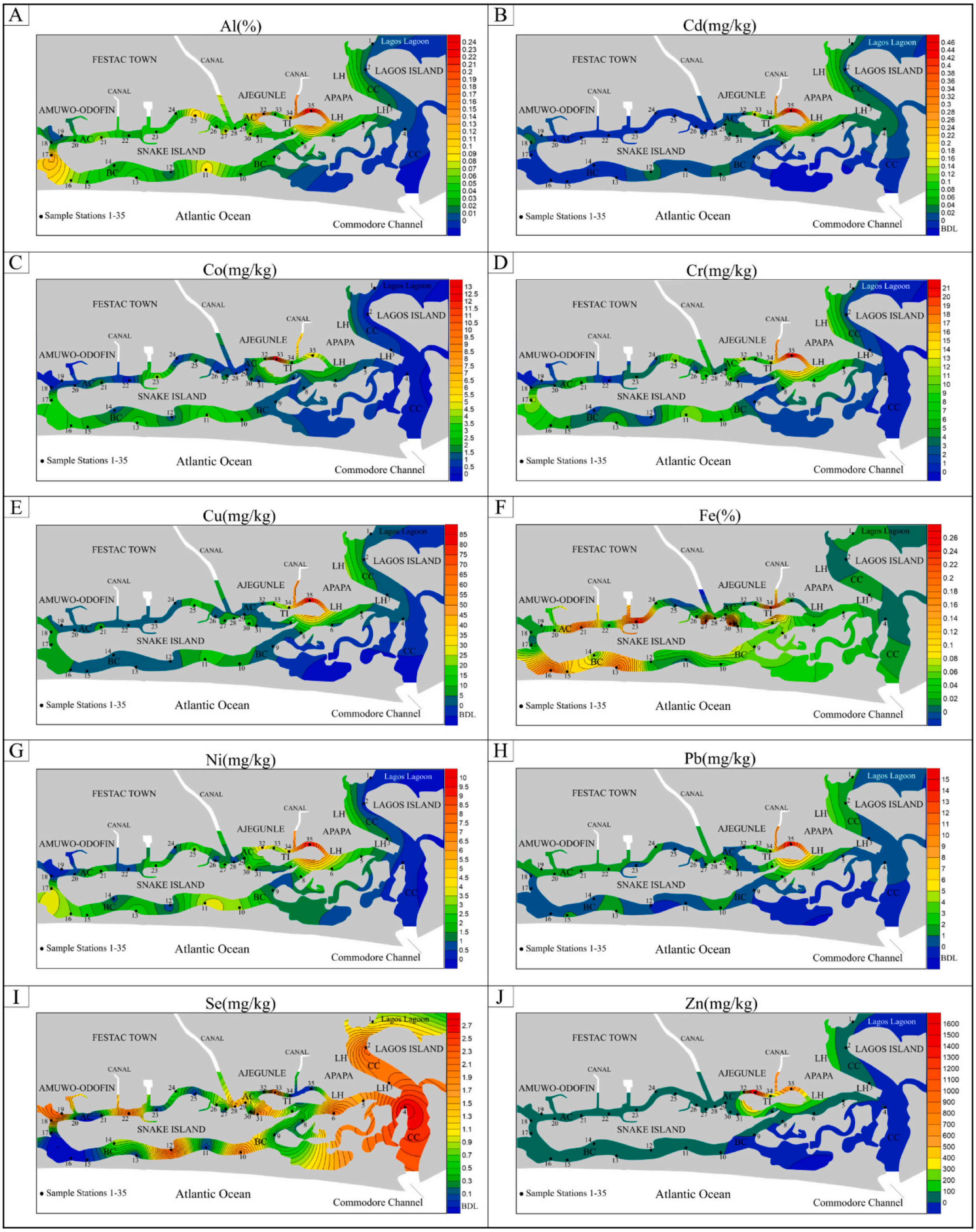

Fig. 7. Heat maps showing the spatial distribution of bioavailable PTEs in the F4 oxidizable fraction across the Apapa-Badagry Creek. ((A): Aluminum (Al), (B): Cadmium (Cd), (C): Cobalt (Co), (D): Chromium (Cr), (E): Copper (Cu), (F): Iron (Fe), (G): Nickel (Ni), (H): Lead (Pb), (I): Selenium (Se), (J): Zinc (Zn).

physiochemistry of the water column, sediment characteristics, and benthic foraminiferal faunas. Not all PTEs were present in either the total or in the F1 and F4 fractions in each of the sectors.

No correlations could be established for CC given the very low number of sampled stations ($n = 3$). In the BC sector ($n = 11$; $p = 0.58$ at 0.05 confidence interval), no significant correlations were observed for *A. salsum*. However, *A. aoetana* had several significant positive correlations with Cr (F4 fraction), Cu (total), and Zn (F4 fraction and total). Of the diversity indices, H(S) had a significant positive correlation with Pb (total). Both salinity and pH had significant positive correlations with the diversity indices. In AC ($n = 11$; $p = 0.58$ at 0.05 confidence interval), *A. salsum* and *Trochammina* sp. 1. had no significant correlations with any of the parameters of interest. More positive and significant correlations were observed for *A. aoetana*. The species correlated positively with the total concentrations of Pb-Cr-Cu-Ni and with Fe-Cu-Zn in the F4 fraction. In addition, it also correlated positively with TOC, CO_3, and mud content. H(S) had a positive correlation with pH and a negative one with TOC, CO_3, Pb-Al-Cu (total), Cu-Zn (F4 fraction).

No correlations were observed for the PTEs dissolved in water except for phosphorous which had a significant negative correlation with S along AC (see Supplemental Material-Appendix E).

4. Discussion

Since the opening of the Lagos Lagoon (east of ABC) in the early 1909, the port development has taken a drastic move with breakthrough at the Apapa Port in 1921, leading to the construction of the first four deep-water berths in the area. The arrival of an army of settlers from the Americas and hinterland country, urbanization and port development, and varying political spaces have propelled Lagos into an outstanding port city in the Gulf of Guinea (Olukoju, 2004, 2014). Further developments came when Lagos was officially declared the capital of independent Nigeria in 1960. The build-up of the city took place as a result of the industrial and residential expansion around the LH environments. Activities such as dredging, indiscriminate waste and sewage disposal, removal of mangroves, and creation of new land areas for human settlements through sand filling and remobilization have sharpened the study area over the years. Given the significant level of anthropogenic alteration of the LH, the overall level of pollution is varied (CF and EF indices). The current impact to the biota is low (RI $<$150) which also includes the stained (living) benthic foraminifera.

4.1. Total PTE sediment geochemistry

The spatial distribution of PTE concentrations varied among the three sectors suggesting different non-point sources of pollution. Several stations with the highest concentrations are considered PTE depocenters. In the case of BC, stations 11 and 17 are depocenters for Co-Cr-Cu-Ni-Zn. Station 11 ("moderately" polluted) is located south of a heavily populated residential area on the southeastern portion of Snake Island while station 17 ("unpolluted") is adjacent to the Bassa residential area on the western tip of the island (Figs. 1 and 5). Although the water depth at these two depocenters are at extremes (1.2 vs 5.2 m), both % mud and TOC are the third and second highest respectively. In the case of Pb, stations 9 ("unpolluted") and 10 ("severely") are depocenters for this pollutant where they show similar water depths but very drastic differences in %mud and TOC values. A general observation is that these PTEs are sequestered and complexed with mud-sized sediments and organic matter respectively in addition to co-precipitating during CO_3 and iron-oxide formation as evidenced by their significant and positive cross correlations. Additionally, those positive correlations with Fe suggests redox conditions at the sediment-water interface (e.g., Martínez-Colón et al., 2009; Martínez-Colón et al., 2018; Castelo et al., 2021; Fajemila et al., 2022a).

The work of Obi et al. (2016) is the only study reporting total PTE concentrations, but unfortunately it was a composite of six sampled sites along the south shoreline of Tincan Island. They reported higher Co-Cr-Cu-Ni-Pb-Zn concentrations in LH when compared to other sites (high urban and industrial activities) in LL (east of ABC). To assess the level of impact of PTEs on benthic organisms, the effect range low (ERL- little to no effects to benthic biota) and effect range median (ERM- adverse effects to benthic biota) sediment quality guidelines (SQG), as stipulated by Long et al. (1995), were implemented. All the PTEs had concentrations < ERL indicative of no adverse effects. The exception being for Cr in stations 11 and 17 (depocenters), whose values were between ERL and ERM indicative of potential adverse effects.

Numerous canals drain into the highly impacted AC (Fajemila et al., 2022b) and serve as non-point sources of pollution. For example, a very small canal draining the Ajegunle urban area is a non-point source of pollution as it discharges its effluents at station 33. This site is considered as "moderately" impacted (CF values) by Co-Pb-Cu and "high" with respect to Zn or as "severely" for Co and "extreme" for Zn (EF values) as it also serves as a depocenter for only Co-Zn. These two PTEs in the organic-bound F4 fraction have a strong positive correlation with TOC suggesting that the high amount of organic matter (7.73 %) served as a sink given the high affinity of PTEs being sequestered and complexed with organic matter. In terms of SQG, Cu-Cr-Ni exceeded ERL, as did Pb at its depocenter (station 35). Zinc is the PTE in this study to have exceeded ERM values, indicating that adverse effects will occur to benthic organisms at its depocenter in station 33.

Similarly, a much bigger canal between Ajegunle and Apapa (Fig. 1) drains between stations 34–35. Given the fate and transport (e.g., eastward surface water current), the highest total concentrations of several PTEs are found in a depocenter in station 35, where it is surrounded by highly urban-industrial complexes in Apapa and Ajegunle to the north and the highly industrialized Tincan Island to the south. Heat maps of total concentrations illustrate this canal to be a non-point source of pollutants. Station 35 is also very shallow (1.4 m) and unlike the BC depocenters, it has the highest percentage of TOC (8.94). This site is considered "moderately" impacted by Cr-Cu and "high" with respect to Pb-Zn based on CF values. It is impacted "moderately" for Co-Fe, "severely" for Cr-Cu, and "high" for Pb-Zn. Like station 33, organic matter served as a sink of these PTEs. Station 35 had the second-highest amount of %mud (83.90 %), and no significant correlations were observed between %mud and the PTEs in the sediment-bound F1 fraction. This is because of the significant and positive correlation between %mud and TOC and the lack of Al, suggesting that the %mud content is dominated more by mud-size organic matter than by lithic minerals. This potentially allows the PTEs to be preferentially complexed by organic matter and, to a lesser amount, to be adsorbed to the surfaces of mud-size lithic sediments. For Pb, a different scenario is proposed given that it showed no correlation with %mud, although a significant positive correlation with TOC and CO_3 was found. This could indicate that Pb is found in other sediment compartments or fractions not analyzed in this study given their limited bioavailability to the foraminifers. For example, it is inferred that Pb co-precipitated with non-bioavailable carbonate minerals (e.g., cerussite- $PbCO_3$), given its significant positive correlation with CO_3 content. Similarly, this PTE could be associated with other mineral (e.g., aluminosilicates) phases based on its positive correlation with Al. This could explain the lack of significant correlations with both the F1 and F4 fractions.

Given the close proximities of the canals to the two depocenters identified along AC, and based on the PTE spatial distributions, it is concluded that the source of Co-Zn is the Ajegunle residential area (north of station 33) and that Cr-Cu-Ni-Pb comes directly from Apapa (north of station 35). This is confirmed not only by their distributions along the harbor (Fig. 8) but also by the fact that no depocenters are found between stations 27–29. Here a big canal located between the Festac Town and Ajegunle drains into those sites.

In comparison to AC and BC, the CC may be a less impacted area, with no depocenters observed and with all PTEs below ERL values as it was expected. This channel is the main conduit of marine waters to both BC and AC, and it is not considered a source of pollutants.

4.2. Benthic foraminifera and PTE bioavailability

Based on the work of Ballendux (n.d.), sea water coming from CC has found its way into the harbor. Although no information was provided regarding the westward-most movement of the sea water bottom current, our data corroborates that the seawater has reached the western shore of Snake Island (Fig. 1) where bottom salinities at stations 17–18 are mesohaline (6.1–6.31). The source of organic matter was interpreted to be from terrestrial sources by Fajemila et al. (2022b) as evidenced by mangrove forests surrounding the portions of the studied area. Also, the terrestrial sediments found in ABC are continentally derived given the presence of kaolinite, illite and montmorillonite clays in addition to a

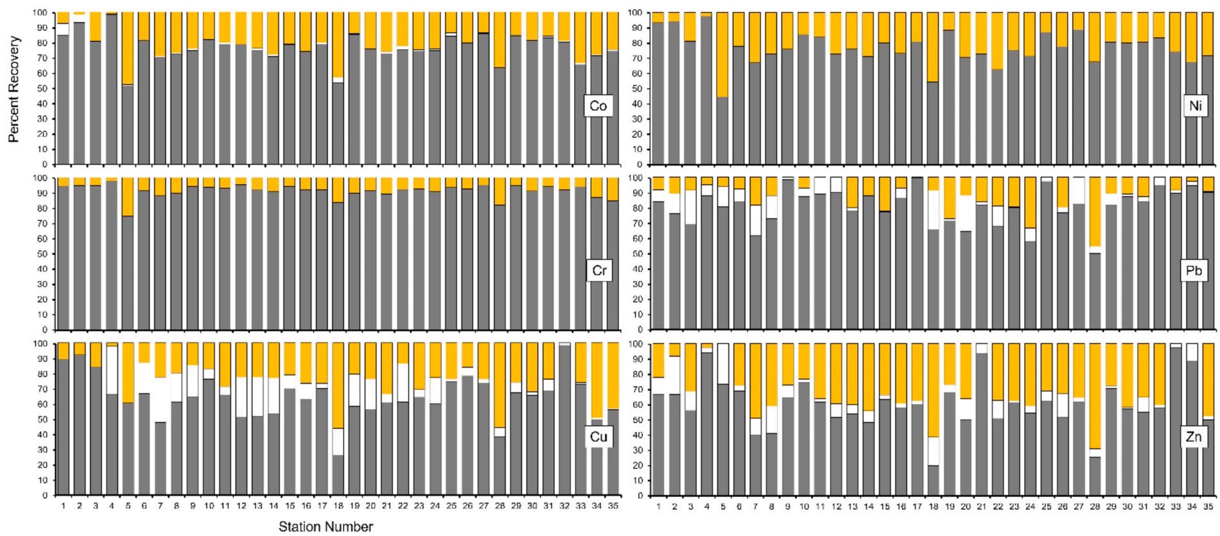

Fig. 8. PTEs percent contribution. Gray = total concentration. White = F1 fraction. Yellow = F4 fraction. (For interpretation of the references to color in this figure legend, the reader is referred to the web version of this article.)

predominant eastward transport (freshwater suspension) of sediments along AC and BC (Ballendux, n.d.).

Benthic foraminiferal distribution in the ABC is similar to that in other nearshore environments in the Gulf of Guinea (e.g., Langer et al., 2016a, 2016b; Fajemila and Langer, 2016; Fajemila et al., 2020). The presence or dominance of *A. aoteana* and *A. salsum* at different sectors in the ABC is controlled by the marine influence (see Jorissen et al., 2022). This is further clarified by the Q-mode cluster dendrogram (Fig. 3). Clusters E and F with sample stations mostly within AC and CC are dominated by species of *Ammonia*, while *A. salsum* is very prominent in Cluster B, which comprises most BC stations. Foraminiferal distribution in the ABC is possibly controlled by salinity and pH, as was the case further east in the LL and several other lagoons and estuaries in west Africa (Debenay et al., 1989).

Dissolved P is an important element (nutrient) which is having a negative impact on S (negative correlation) (see Supplementary Material-Appendix E). Although no extensive documentation exists for P in ABC, Onyema and Popoola (2013) reported high concentrations of this element (650–2680 μg/L) at ~2 km south of station 4. A similar concentration was observed in the Lagoon of Venice in Italy when P pollution significantly impacted benthic foraminifers (low S values) (Albani et al., 2007). However, given an inferred "mixing" of both water masses within ABC, it makes sense that along AC, the H(S) distribution is controlled by pH (positive cross correlation) and organic matter (negative cross correlation) as evidenced by numerous fresh water man-made canals (Fig. 1), which drain and transport primarily terrestrial type organic matter into this area. The presence of a limited number of living (Fajemila et al., 2022b) and dead *A. salsum* coupled with hundreds of dead *A. aoetana* is consistent with the positive correlation with TOC, CO_3, and %mud. These two species are dominant in the ABC. In AC, *A. salsum* had no correlation with any PTE, while *A. aoetana* seem to be positively influenced by Fe-Cu-Zn in the organic-bound fraction (F4) as these PTEs are considered micronutrients (e.g., Martínez-Colón et al., 2009; Kaamoush et al., 2022). However, Cu-Zn in the organic-bound fraction is found to have a negative impact on the overall H(S) distribution. Generally, the distribution of benthic foraminifera along the AC was impacted given the high PTE pollution index values. The sediments around the Tincan Island revealed high contamination by Pb and Zn (Figs. 5–7) in sediments that are barren of foraminifera. Moreover, nearly all the PTE concentrations are at their highest in this section of the AC. Living (stained) specimens were not found in stations 33–35 (Fajemila et al., 2022b) and it is suggested that their absence is due to the impacts of PTEs and other anthropogenic activities around the Tincan Island.

In BC, a different scenario is observed. H(S) is controlled by salinity while S is controlled by both pH and salinity with no correlation with TOC or %mud. Along this creek, the highest abundances of *A. salsum* are recorded coupled with the lower abundance of *A. aoetana* (Figs. 2 and 3B). *Ammotium salsum* is prominent westwards into the Ologe Lagoon (Fig. 1), where the saline water almost equals fresh water (Fajemila and Langer, 2016). This is the same scenario for *Miliammina fusca,* another important tolerant species, with very few numbers in the BC. It was surprising to find that *Trochammina* sp. 1., a non-dominant taxon in the ABC, showed a positive correlation with CO_3, %mud, and salinity given that it has a very low abundances of 333 dead individuals in the whole lagoon (200 in BC). Similar findings were found in LL (east of ABC), where these three taxa were primarily controlled by physiochemical parameters (Fajemila et al., 2022a). The influence of tide on the distribution of these species is very minimal and not as profound as salinity. Unlike the ABC, Langer et al. (2016b) documented that shallow-water benthic foraminifera species distributions are related to strong tidal influences within the Akanda estuary of Gabon. *Ammotium salsum* and other agglutinates are prominent at the Mean High Water Neap tides in the *Avicennia germinans* mangrove trees while the calcareous benthics are strongly restricted to the Mean Low Water Neap level within the *Rhizophora racemosa* mangrove trees. In the ABC, both *A. salsum* and *A. aoetana* are associated with *R. racemosa* mangrove trees. A contrasting difference between LL and the ABC harbor is that the latter has a much higher freshwater influence thus resulting in very low H(S) values. Moreover, the distribution of *A. aoetana* seem to be also influenced (positive correlation) by Cr-Zn found in the organic-bound fraction as these could behave as micronutrients. A similar scenario is observed for *Trochammina* sp. 1. with respect to Cu. Unlike in AC, the ecological diversity indices do not seem to be influenced by any PTE.

The foraminiferal distribution reflects relative healthier conditions along CC characterized by more normal marine conditions. This is exemplified by higher S and H(S) values and the overabundance of *Cribroelphidium mirum* and *Hanzawaia* cf. *H. nipponica*. However, station 2 is the only one to be barren and is considered to be "moderately" polluted with respect to Co-Cr-Fe-Zn (EF values) and "severely" polluted for Pb. The more reliable scenario is that this station has very low percentage of mud (3.63 %) and TOC (0.17 %) because of high energy conditions. Tiamiyu (1989) delineated the CC into biofacies based on foraminiferal and sediment data. Similar to his findings, stations 1, 3–4 of our study fall within the harbor edge biofacies and contain the highest abundance of foraminiferal species in sediments with high mud content.

It is important to highlight the significance of PTE bioavailability and non-bioavailability in relation to use of total vs sequentially extracted concentrations. Perin et al. (1997a, 1997b) discussed that using total concentrations does not provide a clear understanding of the ecotoxicological effects of PTEs because it gives all its phases grouped together and without considering its bioavailability. Similarly, Martins et al. (2010) argued that PTEs associated with immobile fractions (part of the total concentration) do not have short-term effects on foraminifers. As further explained by Martínez-Colón et al. (2009, 2018), Martins et al. (2020), and Fajemila et al. (2022b), relying only on total concentrations could provide over-estimations in terms of their effects on foraminifers. Fig. 8 shows the percent contribution of the two fractions reported in this study including the total concentration. It is evident that the highest concentrations were found in the latter which consists of both bioavailable and non-bioavailable PTEs. For example, PTEs co-precipitated with iron oxides (e.g., mineral hematite) or sulphides (e.g., mineral pyrite and galena), or found within the crystalline structure of continentally derived silicate minerals (e.g., quartz, pyroxene), are not readily accessible or bioavailable to the foraminifers. This is especially important when very strong acids such as perchloric ($HClO_4$) are required in the laboratory to extract PTEs from silicate minerals to determine total concentrations.

The need to rely only on bioavailable PTEs in foraminiferal studies in different nearshore environments (e.g., tropical, temperate) merits further understanding. Several questions, and the need for further investigation arise, in the case of significant positive correlations like foraminiferal abundances and total PTE concentrations. Are these correlations real in terms of providing a glimpse of the true scenario of the environment? Are the total PTE concentrations in sediment an accurate representation of environmental bioavailability and its effects on the benthic foraminifers? Is this an actual representation of the ecological response of the foraminifers to PTE total concentrations?

5. Conclusion

The Lagos Harbor is the economic powerhouse of Nigeria. It is surrounded by vast residential and industrial estates which could serve as sources (point and non-point) of pollutants into the surrounding waters. Our study has revealed that Apapa and Badagry creeks show relative differences in foraminiferal distributions coupled with differences in pollutants and physiochemical properties. Therefore, the following conclusions can be made:

i. The AC, which houses most of the activities in the ABC, has the highest degree of pollution (EF and CF) with three main PTEs depocenters (stations 33–35) north of the Tincan Island.
ii. The data suggests that salinity and pH are the main parameters contributing to the foraminiferal distribution along both creeks. The calcareous wall dominating the AC, while the agglutinated taxa are numerous in the BC sediments. The CC has the highest number of species because of more normal marine conditions. However, PTE depocenters do not support living benthic foraminifera and are mostly barren.
iii. Furthermore, the PTEs bound in the most bioavailable (F4) fraction played a negative role in the assemblage distribution fraction, also having a negative impact on diversity. Only P found in solution had a negative impact on S.
iv. This study has shown the importance of using bioavailable PTEs in ecosystem functioning and its importance in its implementation in nearshore shallow water environments.

CRediT authorship contribution statement

Olugbenga T. Fajemila: Funding acquisition; project conceptualization and administration; field work; sample analysis, writing (original, review and editing); **Michael Martínez-Colón**: Supervision of chemical analysis; data analysis; writing (original, review and editing); **Ivory Coucil**: Chemical analysis; writing (review and editing); and **Silvia Spezzaferri**: project co-administration; writing (review and editing).

Declaration of competing interest

The authors declare the following financial interests/personal relationships which may be considered as potential competing interests:

Olugbenga T. Fajemila reports financial support was provided by Swiss Federation through the Excellence Scholarship. Olugbenga T. Fajemila reports financial support was provided by Tertiary Education Trust Fund Nigeria.

Data availability

Data will be made available on request.

Acknowledgement

This work was supported by the Swiss Government Excellence Scholarship awarded to Olugbenga T. Fajemila (grant number: 20200786); and the Tertiary Education Trust Fund Nigeria awarded to Olugbenga T. Fajemila (grant number: TETFund/16b/0014). Special thanks to Mr. Ayoola Fadiora who helped during field sampling.

Appendix A. Supplementary data

Supplementary data to this article can be found online at https://doi.org/10.1016/j.marpolbul.2022.114359.

References

Ajao, E.A., 1996. Review of the state of pollution of Lagos Lagoon. In: Nigerian Institute of Oceanography and Marine Research, Technical Paper, 106, pp. 1–20.
Albani, A., Barbero, R.S., Donnici, S., 2007. Foraminifera as ecological indicators in the Lagoon of Venice, Italy. Ecological Indicators. https://doi.org/10.1016/j.ecolind.2006.01.003.
Al-Enezi, E., Francescangeli, F., Balassi, E., Borderie, S., Al-Hazeem, S., Al-Salameen, F., Boota Anwar, A., Pawlowski, J., Frontalini, F., 2022. Benthic foraminifera as proxies for the environmental quality assessment of the Kuwait Bay (Kuwait, Arabian Gulf): morphological and metabarcoding approaches. Sci. Total Environ. 833, 155093.
Amao, A.O., Qurban, M.A., Kaminski, M.A., Joydas, T.V., Manikandan, P.K., Frontalini, F., 2019. A baseline investigation of benthic foraminifera in relation to marine sediments parameters in western parts of the Arabian Gulf. Mar. Pollut. Bull. 146, 751–766.
Ballendux, n.d.Ballendux, V.W.H.M. (n.d.), Unpublished Results. On the morphodynamical of Lagos Harbour: An exploratory study of the tidal system. Msc Thesis, Delft University of Technology, p. 131.
Barik, S.S., Singh, R.K., Tripathy, S., Farooq, S.H., Prusty, P., 2022. Bioavailability of metals in coastal lagoon sediments and their influence on benthic foraminifera. Sci. Total Environ. 825, 153986.
Bergamin, L., Romano, E., Finoia, M.G., Venti, F., Bianchi, J., Colasanti, A., Ausili, A., 2009. Benthic foraminifera from the coastal zone of Baia (Naples, Italy): assemblage distribution and modification as tools for environmental characterisation. Mar. Pollut. Bull. 59, 234–244.
Castelo, W.F.L., Alves Martins, M.V., Martínez-Colón, M., Guerra, J.V., Dadalto, T.P., Terroso, D., Filgeuiras Soares, M., Frontalini, F., Duleba, W., Aguilera Socorro, O.A., Geraldes, M.C., Rocha, F., Bergmaschi, S., 2021. Disentangling natural vs. Anthropogenic induced environmental variability during the Holocene: Marambaia Cove, SE sector of the Sepetiba Bay SE Brazil. Environ. Sci. Pollut. Res. https://doi.org/10.1007/s11356-020-12179-9.
Cavaliere, M., Barrenechea Angeles, I., Montresor, M., Bucci, C., Brocani, L., Balassi, E., Margiotta, F., Francescangeli, F., Bouchet, V.M.P., Pawlowski, J., Frontalini, F., 2021. Assessing the ecological quality status of the highly polluted bagnoli area (Tyrrhenian Sea, Italy) using foraminiferal eDNA metabarcoding. Sci. Total Environ. 790, 147871.
Coccioni, R., Frontalini, F., Marsili, A., Mana, D., 2009. Benthic foraminifera and trace element distribution: a case-study from the heavily polluted lagoon of Venice (Italy). Mar. Pollut. Bull. https://doi.org/10.1016/j.marpolbul.2009.08.009.
Davaud, E., Septfontaine, M., 1995. Post-mortem onshore transportation of epiphytic foraminifera: recent example from the tunisian coastline. J. Sediment. Res. A65, 136–142.
Debenay, J.-P., Pages, J., Diouf, P.S., 1989. Ecological zonation of the hyperhaline estuary of the Casamance River (Senegal): foraminifera, zooplankton and abiotic variables. Hydrobiologia 174, 161–176.

Dimiza, M.D., Triantaphyllou, M.V., Portela, M., Koukousioura, O., Karageorgis, A.P., 2022. Response of Living Benthic Foraminifera to Anthropogenic Pollution and Metal Concentrations in Saronikos Gulf (Greece, Eastern Mediterranean). Minerals. https://doi.org/10.3390/min12050591.

Don-Pedro, K.N., Oyewo, E.O., Otitoloju, A.A., 2004. Trend of heavy metal concentrations in Lagos lagoon ecosystem, Nigeria. West Afr. J. Appl. Ecol. 5, 103–114.

El Kateb, A.Stalder, Rueggeberg, A., Neururer, C., Spangenberg, J.E., Spezzaferri, S., 2018. Impact of industrial phosphate waste discharge on the marine environment in the Gulf of Gabes (Tunisia). PLoS. https://doi.org/10.1371/journal.pone.0197731.

El Kateb, A., Beccari, V., Stainbank, S., Spezzaferri, S., Coletti, G., 2020. Living (stained) foraminifera in the Lesser Syrtis (Tunisia): influence of pollution and substratum. PeerJ. https://doi.org/10.7717/peerj.8839.

Elshanawany, R., Ibrahim, M.I., Frihy, O., Abodia, M., 2018. Foraminiferal evidence of anthropogenic pollution along the Nile Delta coast. Environ. Earth Sci. 77, 444.

Fajemila, O.T., Langer, M.R., 2016. Ecosystem indicators: foraminifera, thecamoebians and diatoms from the Ologe Lagoon. Nigeria. Rev. Micropaleontol. 59, 397–407. https://doi.org/10.1016/j.revmic.2016.09.002.

Fajemila, O.T., Langer, M.R., 2017. Spatial distribution and biogeographic importance of foraminiferal assemblages from Sao Tome and Principe, gulf of Guinea, West Africa. N. Jb. Geol. Paläont. (Abh.) 285 (3), 337–360.

Fajemila, O.T., Langer, M.R., Lipps, J.H., 2015. Spatial patterns in the distribution, diversity and abundance of benthic foraminifera around Moorea (Society Archipelago, French Polynesia). PLoS One. https://doi.org/10.1371/journal.pone.0145752.

Fajemila, O.T., Sariaslan, N., Langer, M.R., 2020. Spatial distribution of benthic foraminifera in the Lagos lagoon (Nigeria): tracing the impact of environmental perturbations. PLoS One. https://doi.org/10.1371/journal. pone.0243481.

Fajemila, O.T., Martínez-Colón, M., Sariaslan, N., Council, I.S., Kolawole, T.O., Langer, M.R., 2022a. Contamination levels of potentially toxic elements and foraminiferal distribution patterns in Lagos lagoon: a correlation analysis. Water. https://doi.org/10.3390/w14010037.

Fajemila, O.T., Martínez-Colón, M., Spangenberg, J.E., Spezzaferri, S., 2022b. Organic matter source and distribution in the estuarine Apapa-Badagry Creek, Nigeria: implications for living (stained) benthic foraminiferal assemblage. Mar. Micropaleontol. 172, 102112.

Frontalini, F., Coccioni, R., 2008. Benthic foraminifera for heavy metal pollution monitoring: a case study from the Central Adriatic Sea coast of Italy. Estuar. Coast. Shelf Sci. https://doi.org/10.1016/j.ecss.2007.07.024.

Gildeeva, O., Akita, L.G., Biehler, J., Frenzel, P., Alivernini, M., 2021. Recent brackish water foraminifera and ostracoda from two estuaries in Ghana, and their potential as (palaeo) environmental indicators. Estuar. Coast. Shelf Sci. 256, 107270.

Guo, Y., Mei, X., Meng, X., Lan, X., Chen, H., Yang, H., 2020. Benthic foraminifera and its response to heavy metal pollution: a case study from Liaodong Bay, China. Marine Pollution Bulletin. https://doi.org/10.1016/j.marpolbul.2020.111084.

Hammer, Ø., Harper, D.A.T., Ryan, P.D., 2001. PAST: paleontological statistics software package for education and data analysis. Palaeontol. Electron. 4 (1), 9p.

Jorissen, F.J., 1999. Benthic foraminiferal microhabitats below the sediment-water interface. In: Sen Gupta, B.K. (Ed.), Modern Foraminifera. Kluwer Academic Publishers, Boston, pp. 161–179.

Jorissen, F.J., Fouet, M.P.A., Singer, D., Howa, H., 2022. The marine influence index (MII): a tool to assess estuarine intertidal mudflat environments for the purpose of foraminiferal biomonitoring. Water. https://doi.org/10.3390/w14040676.

Kaamoush, M., El-Agawany, N., Omar, M.Y., 2022. Environmental toxicological evaluation (in vitro) of copper, zinc and cybutryne on the growth and amino acids content of the marine alga Dunaliella Salina. Egyptian J. Aquat. Res. https://doi.org/10.1016/j.ejar.2022.07.004.

Langer, M.R., 1993. Epiphytic foraminifera. Mar. Micropaleontol. https://doi.org/10.1016/0377-8398(93)90035-V.

Langer, M.R., Lipps, J.H., 2006. Assembly and persistence of foraminifera introduced mangroves on Moorea, French Polynesia. Micropaleontology 52, 343–355.

Langer, M.R., Mouanga, G.H., Fajemila, O.T., 2016a. Shallow-water nearshore benthic foraminifera assemblages from Gabon. Micropaleontology 62 (1), 69–80.

Langer, M.R., Fajemila, O.T., Mannl, S., 2016b. Assemblages of recent intertidal mangrove foraminifera from the Akanda National Park, Gabon: sea level proxies preserved in faunal assemblages. N. Jb. Geol. Paläont. (Abh.) 281 (3), 327–338.

Li, T., Cai, G., Zhang, M., Li, S., Nie, X., 2021. The response of benthic foraminifera to heavy metals and grain sizes: A case study from Hainan Island, China. Marine Pollution Bulletin 167, 112328.

Liaghati, T., Preda, M., Cox, M., 2003. Heavy metal distribution and controlling factors within coastal plain sediments, bells creek catchments, Southeast Queensland, Australia. Environ. Int. 29, 935–948.

Long, E.R., MacDonald, D.D., Smith, S.L., Calder, F.D., 1995. Incidence of adverse biological effects within ranges of chemical concentrations in marine estuarine sediments. Environ. Manag. 19, 81–97.

Martínez-Colón, M., Hallock, P., Green-Ruíz, C., 2009. Strategies for using shallow-water benthic foraminifers as bioindicators of potentially toxic elements: a review. J. Foraminifer. Res. 39, 278–299.

Martínez-Colón, M., Hallock, P., Green-Ruíz, C., Smoak, J.M., 2017. Temporal variability in potentially toxic elements (PTE's) and benthic foraminifera in an estuarine environment in Puerto Rico. Micropaleontology 63, 357–381.

Martínez-Colón, M., Hallock, P., Green-Ruíz, C., Smoak, J.M., 2018. Benthic foraminifera as bioindicators of potentially toxic element (PTE) pollution: torrecillas lagoon (San Juan Bay Estuary), Puerto Rico. Ecol. Indic. 89, 516–527.

Martins, V., Silva, E.F.D., Sequeira, C., Rocha, F., Duarte, A.C., 2010. Evaluation of the ecological effects of heavy metals on the assemblages of benthic foraminifera of the canals of Aveiro (Portugal). Estuarine Coast. Shelf Sci. https://doi.org/10.1016/j.ecss.2010.01.011.

Martins, M.V.A., Silva, F., Lazaro, L.M.L., Frontalini, F., Clemente, I.M., Miranda, P., Figueira, R., Sousa, S.H.M., Dias, J.M.A., 2015. Response of benthic foraminifera to OM quantity and quality and bioavailable concentrations of metals in Aveiro lagoon (Portugal). PLoS One 10 (2), e0118077.

Martins, M.V.A., Helali, M.A., Zaaboub, N., Boukef-BenOmrane, I., Frontalini, F., Reis, D., Portela, H., Clemente, Matos Morea, Nogueira, L., Pereiro, E., Miranda, P., El Bour, M., Aleya, L., 2016. OM quantity and quality, metals availability and foraminifera assemblages as environmental proxy applied to the Bizerte lagoon (Tunisia). Mar. Pollut. Bull. 105, 161–179.

Martins, M.V.A., Hohenegger, J., Martínez-Colón, M., Frontalini, F., Bergamashi, S., Laut, L., Belart, P., Mahiques, M., Pereira, E., Rodrigues, R., et al., 2020. Ecological quality status of the NE sector of the Guanabara Bay (Brazil): a case of living benthic foraminiferal resilience. Mar. Pollut. Bull. 158, 111449.

Montagna, P., Palmer, P., Pollack, J., 2013. Hydrological changes and estuarine dynamics. In: Springer Briefs in Environmental Science. https://doi.org/10.1007/978-1-4614-5833-3.

Obi, C.C., Adebusoye, S.A., Ugoji, E.O., Ilori, M.O., Amund, O.O., Hickey, W.J., 2016. Microbial communities in sediments of Lagos Lagoon, Nigeria: ellucidation of community structure and potential impacts of contamination by municipal and industrial wastes. Frontiers in Microbiology. https://doi.org/10.3389/fmicb.2016.01213. PMID: 27547200.

Olukoju, A., 2004. The Liverpool of West Africa: The Dynamics and Impact of Maritime Trade in Lagos, 1900–1950. Africa World Press, Trenton, NJ.

Olukoju, A., 2014. The Port of Lagos, 1850–1929: therise of West Africa's leading seaport. In: Bosa, M.S. (Ed.), Atlantic Ports and the First Globalisation, c. 1850–1930. Cambridge Imperial and Post-Colonial Studies Series. Palgrave Macmillan, London. https://doi.org/10.1057/9781137327987_6.

Onyema, I.C., Popoola, R.T., 2013. The physico-chemical characteristics, chlorophyll a levels and phytoplankton dynamics of the east mole area of the Lagos Harbour, Lagos. Journal of Asian Scientific Research 3 (10), 995–1010.

Parker, W.C., Arnold, A.J., 1999. Quantitative methods of data analysis in foraminiferal ecology. In: Sen, G.B.K. (Ed.), Modern Foraminifera. Kluwer, Dordrecht, The Netherlands, pp. 71–89.

Perin, G., Bonardi, M., Fabris, R., Simoncini, B., Manente, S., Tosi, L., Scotto, S., 1997a. Heavy metal pollution in Central Venice lagoon bottom sediments: evaluation of the metal bioavailability by geochemical speciation procedure. Environ. Technol. 18 (6), 593–604.

Perin, G., Fabris, R., Wegener, A.R., Hamacher, C., Manente, S., Tosi, L., Scotto, S., 1997b. A five-year study on the heavy-metal pollution of Guanabara Bay sediments (Rio de Janeiro, Brazil) and evaluation of the metal bioavailability by means of geochemical speciation. Water Res. 31, 3017–3028.

Pinto, E., Sigaud-Kutner, T.C.S., Leitão, M.A.S., Okamoto, O.K., Morse, D., Colepicolo, P., 2003. Heavy metal–induced oxidative stress in algae. J. Phycol. 39 (6), 1008–1018.

Sariaslan, N., Langer, M.R., 2021. Atypical, high-diversity assemblages of foraminifera in a mangrove estuary in northern Brazil. Biogeosciences 18, 4073–4090.

Schönfeld, J., Alve, E., Geslin, E., Jorissen, F.J., Korsun, S., Spezzaferri, S., Members of the FOBIMO group, 2012. The FOBIMO (Foraminiferal Bio-monitoring) initiative – Towards a standardized protocol for soft-bottom benthic foraminiferal monitoring studies. Marine Micropaleontology 94–95, 1–13.

Sen Gupta, B.K., 2013. The roots of environmental micropalaeontology: early inquiries into modern foraminiferal distributions. In: Bowden, A.J., Gregory, F.J., Henderson, A.S. (Eds.), Landmarks in Foraminiferal Micropalaeontology: History and Development. https://doi.org/10.1144/TMS6.14.

Shannon, C.E., 1948. A mathematical theory of communication. Bell Syst. Tech. J. https://doi.org/10.1002/j.1538-7305.1948.tb01338.x.

Tessier, A., Campbell, P.G.C., Bisson, M., 1979. Sequential extraction procedure for the speciation of particulate trace metals. Anal. Chem. 51, 844–851.

Tiamiyu, A., 1989. Ecology and distribution of foraminifera in Lagos Harbour, Nigeria. J. Min. Geol. 25 (1–2), 183–198.

Turekian, K.K., Wedepohl, K.H., 1961. Distribution of elements in some major units of the earth's crust. Geol. Soc. Am. Bull. 72, 175–192.

U.S. EPA, 2007. Method 3051A (SW-846): Microwave Assisted Acid Digestion of Sediments, Sludges, and Oils. Washington, DC, 30p. https://www.epa.gov/sites/production/files/2015-12/documents/3051a.pdf.

Vijverberg, T., Reneerkens, M., Winterwerp, H., Scholl, O., Haruna, Y., 2012. Sediment dynamics in Lagos harbour- reconnaissance on effects of dredging. Coast. Eng. Proc. https://doi.org/10.9753/icce.v33.sediment.75.

Yanko, V., Ahmad, A., Bresler, V., 1998. Morphological deformities of benthic foraminiferal tests in response to pollution by heavy metals: implications for pollution monitoring. J. Foraminifer. Res. 28, 177–200.